

Quantum-confined Stark effect on spatially indirect excitons in CdTe/Cd_xZn_{1-x}Te quantum wells

H. Haas and N. Magnea

Département de Recherche Fondamentale sur la Matière Condensée, CEA-Grenoble, SP2M/PSC, 38054 Grenoble, Cedex 9, France

Le Si Dang

Laboratoire de Spectrométrie Physique, Université J. Fourier-Grenoble I, Boîte Postale 87, 38402 Saint Martin d'Hères, France

(Received 21 March 1996)

The quantum-confined Stark effect is studied in the mixed type-I/type-II CdTe/Cd_xZn_{1-x}Te strained heterostructures. The type-II nature of the light-hole excitons is unambiguously confirmed by the blueshift observed under increasing electric field, in good agreement with calculations. On the other hand, the heavy-hole excitons are redshifted as expected for type-I excitons. The peculiar valence-band alignment, resulting from the sign reversal of the strain between the wells and the barriers, is used to detect the electric-field induced mixing of LH₁ and HH₂ confined hole states. An accurate value for the long-disputed chemical valence-band offset of CdTe/ZnTe system is extracted as $\Delta E_V = (11 \pm 3)\%$ of the band-gap difference between unstrained CdTe and ZnTe materials. [S0163-1829(96)06835-X]

The CdTe/Cd_xZn_{1-x}Te quantum-well (QW) system offers unique physical properties due to the difference in lattice parameter between CdTe and ZnTe which alters considerably the band alignment of the heterostructure because of the relatively small valence-band offset (VBO) in the absence of strain. But, while the deformation potentials a_c , a_v , and b linking the strain to the band structure are relatively well known,¹ the “chemical” VBO has not yet been accurately determined and different values ranging between 0% and 20% have been proposed.^{2,3} As shown in Fig. 1 depicting the band structure under a 10-kV/cm electric field for a VBO of

11%, the strain of opposite sign in the barrier and in the QW induces a type-II band structure for light holes which are confined in the Cd_xZn_{1-x}Te barriers whereas the heavy holes are confined in the same layer as the electrons (type-I band structure). This configuration is possible only if the strain contribution is superior to the chemical VBO.² This can be checked by the measurement of the quantum-confined Stark effect (QCSE) which allows one to determine unambiguously the valence-band configuration. Indeed, by applying a longitudinal electric field it will be easy to check the nature of electron–light-hole transitions because type-II excitons are expected to shift linearly to the blue whereas type-I transitions should redshift quadratically.⁴ The goal of this paper is to describe experimental measurements of the QCSE obtained on Schottky diodes and calculations which allow us to determine the nature of the excitons and the band lineup in the CdTe/Cd_xZn_{1-x}Te system. These results add new insights about the behavior of mixed type-I systems, such as InAs/GaAs, already studied.⁵

The samples are grown by molecular-beam epitaxy on (001) Cd_{0.75}Zn_{0.25}Te substrates transparent at the energy of the excitons in CdTe quantum wells. The use of this special substrate with a lattice parameter situated between those of the QW (CdTe) and the barrier (Cd_{0.62}Zn_{0.38}Te) allows pseudomorphic growth of strain symmetrized structures.⁶ An *n*-type strain-free Cd_{0.75}Zn_{0.25}Te indium-doped layer ($n = 10^{17} \text{ cm}^{-3}$) of 1.5 μm thickness is grown first, providing a buried electrical contact layer. The multiple QW's (MQW's) are made up of 40 periods of 81-Å CdTe and 104 Å of Cd_{0.62}Zn_{0.38}Te layers as deduced from x-ray diffraction measurements. The MQW region is embedded in a Schottky diode, formed by a semitransparent gold film deposited on top of the cap layer and the buried *n*-type doped layer. Standard photolithography is used to produce circular diodes of 1 mm diameter. A chemical etch give access to the doped layer which is contacted Ohmically by evaporation of indium. The wide transparent spectral range of the substrate allows us to measure directly the transmission of the samples. We define

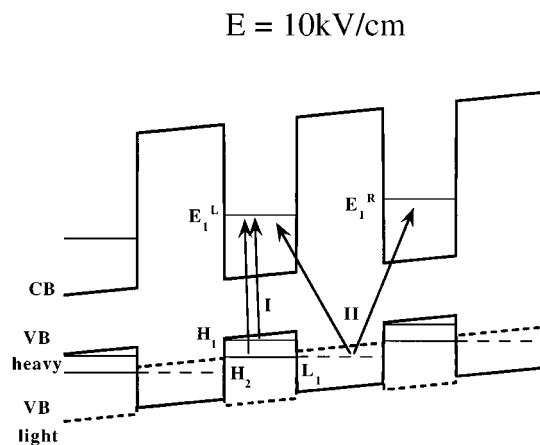


FIG. 1. Calculated band structure of CdTe/Cd_{0.62}Zn_{0.38}Te multiple quantum wells under a 10-kV/cm electric field showing electron ($E_1^{\text{left}}, E_1^{\text{right}}$), heavy-hole (H_1, H_2), and light-hole (L_1) confined states. The heavy-hole valence band (full line) and light-hole valence band (dotted line) are split by the lattice mismatch strain imposed by the substrate. The arrows correspond to the type-I ($E_1 H_{1,2}$) and type-II ($E_1^{L,R}, H_1$) absorption transitions. At 10 kV/cm the H_2 heavy-hole state confined in the CdTe quantum well is degenerate with the L_1 light-hole state confined in the Cd_{0.62}Zn_{0.38}Te barrier.

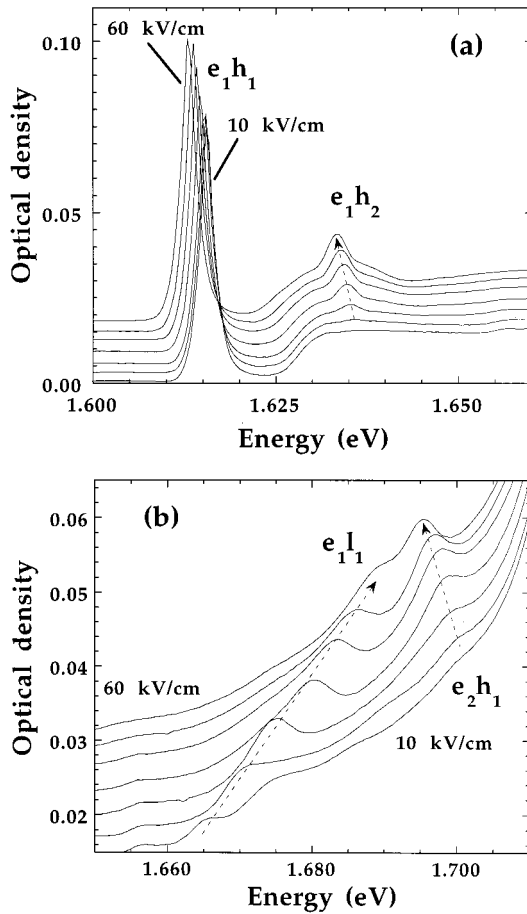


FIG. 2. (a) 2-K excitonic absorption of CdTe/Cd_{0.62}Zn_{0.38}Te multiple quantum well for electric fields varying between 10 and 60 kV/cm in steps of 10 kV/cm showing heavy-hole related lines e_1h_1 and e_1h_2 . The oscillator strength of the parity-forbidden e_1h_2 transition increases with the field. (b) 2-K excitonic absorption of CdTe/Cd_{0.62}Zn_{0.38}Te multiple quantum wells for electric fields varying between 10 and 60 kV/cm for the light-hole related line e_1l_1 . The blueshift of the e_1l_1 line is characteristic of a spatially indirect transition.

the optical density of the samples as the natural logarithm of the transmitted intensity divided by the transmitted intensity in the completely transparent region at lower energy ($h\nu < 1.568$ eV). Electroabsorption experiments are performed at low temperature (2–30 K) with a white lamp source filtered by the substrate which cuts off the highest-energy photons. Photoluminescence and polarized photoluminescence excitation (PPLE) experiments are performed with a Ti-sapphire laser as excitation source.

Typical electroabsorption spectra recorded in the vicinity of the fundamental excitonic transitions are shown in Fig. 2(a) for electric fields varying between 10 and 60 kV/cm. The heavy-hole transitions e_1h_1 and e_1h_2 shift towards lower energies under electric field which is characteristic for the QCSE on type-I QW's. The redshift of the fundamental transition between flat-band conditions and 60 kV/cm is around 5 meV. As expected for a parity-forbidden transition between even and odd states, the e_1h_2 transition gains in oscillator strength because the overlap of the electron and hole wave functions increase under electric field. For the same range of applied electric fields the e_1l_1 transition is

shown in Fig. 2(b). The e_1l_1 transition shifts rapidly to higher energies. It blueshifts nearly linearly by 35 meV between flat-band conduction and 60 kV/cm. For comparison, the redshift of the type-I e_2h_1 transition for the same fields is only 5 meV. Such a fundamental difference can only be explained if the light holes are confined in barriers whereas the heavy holes are confined in the same layer as the electrons.

If we neglect initially the excitonic interaction the energy of transition under an electric field F for a type-I E_nH_m transition can be written

$$E_nH_m = E_g + E_n(F) + HH_m(F) - eFL_W, \quad (1)$$

where $E_n(F)$ and $HH_m(F)$ are the field-dependent confinement energy of electrons and heavy holes in the QW and L_W is the well thickness. The last term of relation (1) explains the redshift of the type-I transitions. For a type-II transition involving light-hole states a different behavior is expected. As shown in Fig. 1, the light-hole state LH₁ can give rise to two transitions: one with an electron to the right of the QW and the other with the electron to the left. These transitions are equivalent in the absence of an electric field. But on electric field the wave function of the light hole LH₁ shifts towards the right interface which gives rise to two kinds of transition differing in their energy:

$$E_n^{\text{right}}L_m = E_g + E_n(F) + LH_m(F), \quad (2a)$$

$$E_n^{\text{left}}L_m = E_g + E_n(F) + LH_m(F) - eF(L_W + L_B). \quad (2b)$$

The $E_1^{\text{right}}L_1$ transition, and thus the e_1l_1 excitonic transition, shifts to the blue due to the increasing carrier confinement in triangular wells (see Fig. 1) and gains in oscillator strength owing to the greater overlap of the wave functions. On the other hand, for the transition $E_1^{\text{left}}L_1$ (e_1l_1' excitonic transition) with the electron confined in the CdTe layer at the left, a large redshift is expected because of the potential drop across the barrier *plus* the well. Since the overlap of the electron and light-hole wave function (already small at zero field) decreases very quickly, this transition has not been observed in the transmission spectra of our samples. Nevertheless it can strongly influence the electronic band structure through band mixing effects as we shall see below.

To confirm the attribution of the e_1l_1 transition to the light-hole subband we have measured the ratio of circular polarization in PPLE under electric field. Because of the presence of photogenerated carriers, the electric field is not given by the value of the applied voltage but is deduced from the shift of the e_1l_1 transition. As shown in Fig. 3(a), at low field we observe a polarization ratio for e_1l_1 opposite to the ones of e_1h_1 and e_1h_2 , attributed to heavy-hole excitons, which indicates clearly that this transition indeed involves light-holes states.⁷ As we increase the electric field, this transition shifts to higher energies as observed previously in the transmission measurements [see Fig. 3(b)] while preserving its negative polarization ratio. Simultaneously, we can also detect the e_1l_2 transition at higher energies.

While the polarization of e_1l_1 remains negative between 5–20 kV/cm, the polarization of the e_1h_2 transition changes its sign, indicating a light-hole character for field higher than 12 kV/cm. This phenomenon might be explained by mixing of the H_2 heavy-hole and L_1 light-hole subbands under elec-

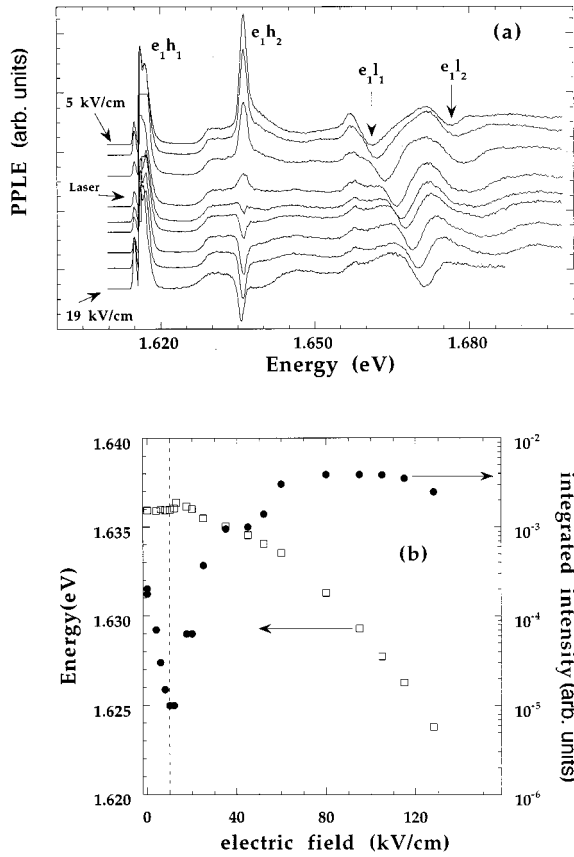


FIG. 3. (a) Circularly polarized photoluminescence excitation spectra of CdTe/Cd_{0.62}Zn_{0.38}Te multiple quantum wells under electric fields of 5 to 19 kV/cm detected on the low-energy side of the e_1h_1 excitonic transition. Positive peaks are attributed to heavy-hole excitons and negative peaks to light-hole excitons. Near 10 kV/cm the sign of the polarization ratio of the e_1h_2 line changes from positive to negative as a result of the mixing between the H_2 and L_1 confined hole states. (b) Electric-field dependence of the energy (empty square) and integrated intensity (full circle) of the e_1h_2 line measured in transmission spectra.

tric field. As seen on Fig. 1 where we have drawn the calculated band structure at 10 kV/cm, the H_2 subband is effectively degenerated with the L_1 subband. These subbands can mix as shown theoretically by Schulman and Chang for GaAs.⁸ In the GaAs/Ga_xAl_{1-x}As case light- and heavy-hole subbands are in the same layer while in our case the interacting subbands are in adjacent layers. Then the e_1h_2 transition will have a light-hole component reflecting the strength of the mixing. On Fig. 3(b) we have plotted the energy shift and the integrated intensity of the e_1h_2 versus the electric field measured in the transmission spectra. In the absence of any coupling we would expect a monotonic increase of the oscillator strength of this parity-forbidden transition along with the redshift. On the contrary, we see an initial decrease of the intensity of the e_1h_2 transition with a minimum near 10 kV/cm, where the light-hole contribution is observed. This transfer of intensity towards the e_1l_1 transition is another indication of the mixing of H_2 and L_1 states. For fields higher than 30 kV/cm the e_1h_2 transition recovers its oscillator strength and probably its heavy-hole character but un-

fortunately we could not exceed 20 kV/cm in PPLE experiments because of the efficient screening of the electric field by the carriers generated by the optical excitation.

The theoretical calculation of the wave functions and the eigenvalues of electron and hole states under electric field is based on the resolution of the Schrödinger equation as in Ref. 9. The physical constants involved in the calculations are given in Ref. 2. The light- and heavy-hole exciton binding energies E_b^X are calculated using the numerical solution of Peyla *et al.*¹⁰ based on the model of Leavitt and Little.¹¹ To get an accurate value of E_b^X we have to include the effect of the longitudinal-optical phonon field on the Coulomb electron-hole interaction. For this purpose we have used the three-dimensional (3D) model of Haken¹² which gives an effective dielectric constant ϵ_{eff} depending on the exciton Bohr radius and on the electron and hole polaron lengths. For an 81-Å-thick QW between Cd_{0.62}Zn_{0.38}Te barriers the fundamental heavy-hole exciton has a calculated exciton binding energy of 19 meV with $\epsilon_{\text{eff}}=9.4$ instead of 10.6. From the $1S-2S$ splitting and using the model of Mathieu, Lefevre, and Cristol¹³ we get an experimental exciton binding energy $E_b^X = 19.5 \pm 0.5$ meV in very good agreement with the calculated value. Similar good agreement is obtained for different well thicknesses and barrier heights, confirming the importance of a correct treatment of the Fröhlich interaction in the calculation of the exciton binding energy especially when E_b^X is close to the LO phonon energy. The electric-field dependence of the exciton binding energy was calculated by a variational method only for the e_1hh_1 and e_1hh_2 transitions as in Ref. 14.

In Fig. 4 we compare the theoretical and experimental shift of the e_nh_m and e_lj excitonic transitions as a function of the electric field. For the heavy-hole transitions e_1h_1 and e_1h_2 , where the field dependence of E_b^X has been included, a good agreement is obtained up to 70 kV/cm. Typically for an electric field of about 10^5 V/cm the calculated exciton binding energy for e_1h_1 is reduced by 4 meV. In comparison the exciton binding energy for e_1h_2 first increases up to 70 kV/cm (1 meV) and then decreases slightly. These results can be explained by the increasing overlap of the wave functions of the first electron level (e_1) and the second hole level (h_2) under electric field. This overlap reaches its maximum around 70 kV/cm. For e_2h_1 this correction has not been carried out but the theoretical curve fits the experimental data quite well. Similarly to the case of e_1h_2 , the exciton binding energy for a transition between an antisymmetric electron wave function and a symmetric hole wave function does not vary too much (around 1 meV) with the electric field.

The measured zero-field energy and the observed blueshift of the light-hole transition e_1l_1 with the electric field is very well reproduced by the calculation for a theoretical light-hole exciton binding energy of 5 meV. The agreement is good up to 40 kV/cm but above that value the observed slowing down of the blueshift could result from an increase of the exciton binding energy as expected for a spatially indirect transition under an electric field.

The complete set of experimental data can now be used to determine precisely the valence-band offset. In Fig. 5 we compare the experimental energy positions at zero field of the e_nh_m and e_lj transitions with the calculated ones for

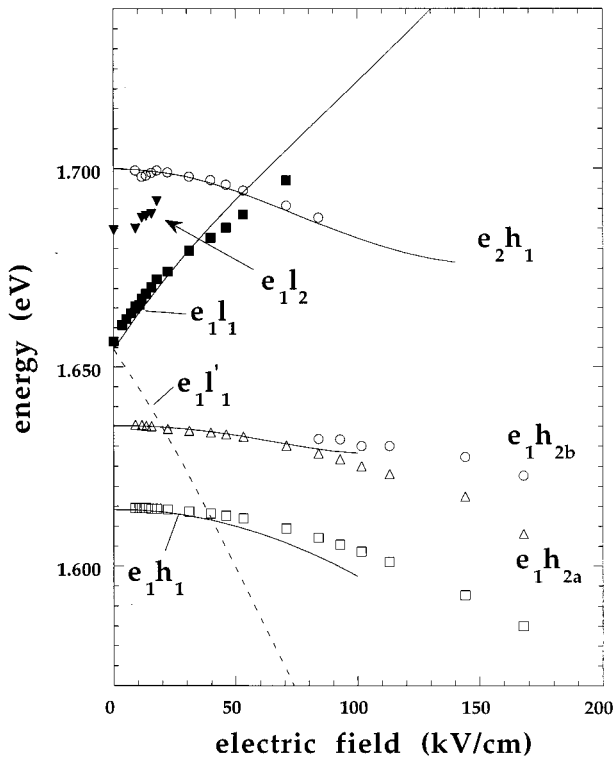


FIG. 4. Experimental positions (symbols) and calculated energies (continuous lines) of the excitonic transitions observed in CdTe/Cd_{0.62}Zn_{0.38}Te multiple quantum well as a function of electric field.

different values of the chemical VBO. The straight line corresponds to the ideal agreement of the calculation with the measured values. The heavy-hole transitions $e_n h_m$ are quite insensitive to the band offset because they are type-I–direct transitions. On the other hand, the type-II–indirect light-hole transitions $e_i l_j$ show an extreme sensitivity to the band-offset value as shown in Fig. 5. This leads to a precise determination of the VBO in this system equal to $(11 \pm 3)\%$ of the band-gap difference between CdTe and ZnTe providing that it is independent of the strain. This result is quite different from our previous determinations where smaller values of the VBO have been obtained.^{2,3} We think that this last value is more reliable than the previous estimates because of the existence in the present structures of a real type-II light-hole exciton. In structures with lower Zn content in the barriers like those used in Refs. 2 and 3, the Coulomb interaction can make the light exciton effectively type I which hinders a precise deduction of the VBO. In a recent experiment we have indeed confirmed that in samples with only 10% Zn in

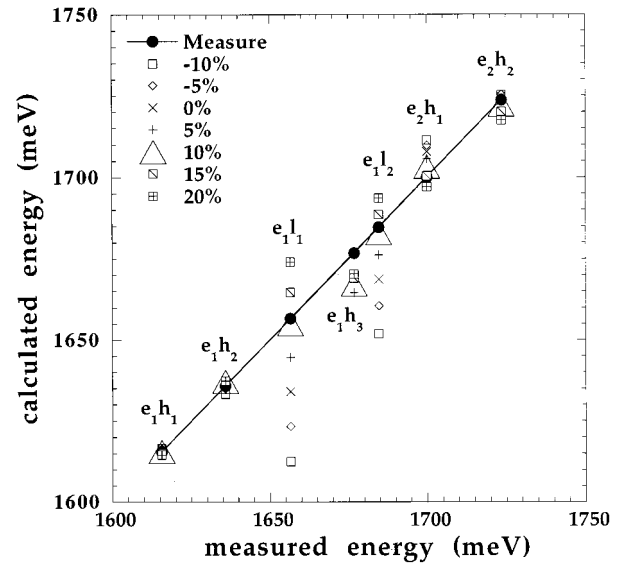


FIG. 5. Plot of the experimental energy position of the excitonic transitions observed in CdTe/Cd_{0.62}Zn_{0.38}Te multiple quantum wells versus the theoretical energy positions calculated for several values of the valence-band offset. The straight line which corresponds to the ideal fit shows that the best agreement between experiment and theory is obtained for a valence-band offset $\Delta E_V = 11\% \Delta E_g$.

the barriers, the $e_1 l_1$ exciton is quasidirect with the light-hole state LH₁ localized in the CdTe wells at zero field but becomes type II above a characteristic electric field of 20 kV/cm. Such a behavior has been predicted and calculated theoretically by Kavokin and Nesvizhskii.¹⁵

In summary the quantum-confined Stark effect has been observed for type-I/type-II CdTe/Cd_xZn_{1-x}Te quantum wells in optical transmission experiments. In structures with sufficient confinement we demonstrate unambiguously that the light-hole exciton transitions are spatially indirect. This peculiarity is used to determine a chemical valence-band offset of $[(11 \pm 3)\%] \Delta E_g$ between ZnTe and CdTe. In these materials the excitonic effects are important and they must be considered in detail. The behavior of the light- and heavy-hole excitonic transitions under an electric field can be understood very well and is reproduced quite accurately by the calculations. By using these results we have been able to design heterostructures exhibiting room-temperature excitonic absorption and efficient electromodulation properties.¹⁶

The authors acknowledge F. Kany, Q. X. Zhao, R. André, N. Pelekanos, R. T. Cox, J. L. Pautrat, and P. Gentile for their help and support during the course of this work.

¹M. Zigone, H. Roux-Buisson, H. Tuffigo, N. Magnea, and H. Mariette, *Semicond. Sci. Technol.* **6**, 454 (1991).

²H. Tuffigo, N. Magnea, H. Mariette, A. Wasiela, and Y. Merle d'Aubigné, *Phys. Rev. B* **43**, 14 629 (1991).

³E. Deleporte, J. M. Berroir, C. Delalande, N. Magnea, H. Mari-

ette, J. Allegre, and J. Calatayud, *Phys. Rev. B* **45**, 6305 (1992).

⁴G. Bastard, E. E. Mendez, L. L. Chang, and L. Esaki, *Phys. Rev. B* **28**, 3241 (1983).

⁵J. Whittaker *et al.*, *Phys. Rev. B* **42**, 3591 (1990).

⁶A. Ponchet, G. Lentz, H. Tuffigo, N. Magnea, H. Mariette, and P.

- Gentile, J. Appl. Phys. **68**, 6229 (1990).
- ⁷Y. Kato, Y. Takahashi, S. Fukatsu, Y. Shiraki, and R. Ito, J. Appl. Phys. **75**, 11 (1994).
- ⁸J. B. Schulman and Y. C. Chang, Phys. Rev. B **31**, 2056 (1985).
- ⁹E. J. Austin and M. Jaros, Phys. Rev. B **31**, 5569 (1985).
- ¹⁰P. Peyla, Y. Merle d'Aubigné, A. Wasiela, H. Mariette, M. D. Struge, N. Magnea, and H. Tuffigo, Phys. Rev. B **46**, 1557 (1992).
- ¹¹R. P. Leavitt and J. W. Little, Phys. Rev. B **41**, 1174 (1990).
- ¹²H. Haken, in *Excitons, Magnons and Phonons, Beirut Symposium*, edited by A. B. Zallen (Cambridge University Press, Cambridge, 1968).
- ¹³H. Mathieu, P. Lefevre, and P. Cristol Phys. Rev. B **46**, 4092 (1992).
- ¹⁴R. André, J. Cibert, and Le Si Dang, Phys. Rev. B **52**, 12 013 (1995).
- ¹⁵A. V. Kavokin and A. I. Nesvizhskii, Phys. Rev. B **49**, 17 055 (1994).
- ¹⁶H. Haas, P. Gentile, N. Magnea, J. L. Pautrat, Le Si Dang, and N. Pelekanos, Mat. Sci. Eng. B **21**, 224 (1993).